

# Influence of quantum size effects on Pb island growth and diffusion barrier oscillations

Shao-Chun Li,<sup>1,2</sup> Xucun Ma,<sup>1</sup> Jin-Feng Jia,<sup>1,\*</sup> Yan-Feng Zhang,<sup>1</sup> Dongmin Chen,<sup>1</sup> Qian Niu,<sup>3</sup> Feng Liu,<sup>4</sup> Paul S. Weiss,<sup>2</sup> and Qi-Kun Xue<sup>1</sup>

<sup>1</sup>*Institute of Physics, Chinese Academy of Sciences, Beijing 100080, China*

<sup>2</sup>*Department of Chemistry and Physics, The Pennsylvania State University, University Park, Pennsylvania 16802, USA*

<sup>3</sup>*Department of Physics, University of Texas at Austin, Texas 78712, USA*

<sup>4</sup>*Department of Material Science and Engineering, University of Utah, Salt Lake City, Utah 84112, USA*

(Received 5 March 2006; revised manuscript received 27 June 2006; published 9 August 2006)

Quantum size effects are successfully exploited in manipulating the growth of (111) oriented Pb islands on Si(111) substrate with a scanning tunneling microscope. The growth dynamics and morphology displayed can be well controlled through the quantum size effects defined by the island thicknesses and the interplay with the classical forces. The transition of growth modes from quantum to classical regime and the quantum beating in morphological dynamics are directly identified in real space and quantitatively analyzed. Atomic diffusion barriers, an important parameter in the thin film growth process, are also demonstrated to be modified by quantum size effects, and oscillate with a two-monolayer periodicity.

DOI: [10.1103/PhysRevB.74.075410](https://doi.org/10.1103/PhysRevB.74.075410)

PACS number(s): 68.55.Jk, 68.37.Ef, 73.21.-b, 81.16.-c

When the sizes of materials are reduced to be comparable to the Fermi wavelength, electrons' energies are quantized and sensitively size-dependent due to the quantum confinement, which are collectively named quantum size effects (QSEs).<sup>1,2</sup> QSEs are well known to play a crucial role in both nanoscience and nanotechnology.<sup>3-9</sup> QSEs can predominate both the formation and stability of thin films in nanoscale. On the other hand, free energy costs from steps provide the usual "classical" driving force to smoothen the film's surface. In general, the classical step effect (CSE) predominates the growth of thicker films,<sup>10-12</sup> and QSE the thinner ones. Okamoto *et al.* have observed the QSE-driven strip flow and double layer growth inside a Pb ring-shaped structure, and the stability of such a ring-shaped structure was qualitatively ascribed to the competition between QSE and classical effect.<sup>7</sup> To date, the interplay between QSE and CSE has not been quantitatively explored due to the difficulty in controlling both factors simultaneously, even though the QSE and the CSE have been extensively studied separately.

For a Pb(111) island grown on a Si(111) substrate, electrons confined in the potential well formed by the vacuum barrier and the energy band gap of the substrate are quantized into quantum well states (QWS). Because the Fermi wavelength of electrons in Pb is nearly four times the interlayer spacing in the [111] direction, the QWS energy, and thus the Pb film stability,<sup>6-8</sup> exhibit oscillations with periods of  $\sim 2$  monolayers (ML). However, for an ultrathin Pb(111) island grown on a stepped Si(111) substrate, a smooth flat surface (wedge shape) favored by CSE is unfavored by QSE because it inevitably contains consecutive even (stable) and odd (unstable) layers (see the schematic in Fig. 1). Consequently, QSE and CSE drive the system in opposite directions, as both are expected to contribute and to compete in the growth process.

In this paper, a manipulation approach is employed to trigger the growth of wedge-shaped Pb islands on stepped Si(111) substrates using a scanning tunneling microscope (STM).<sup>10</sup> The experiment reveals intriguing growth dynamics and morphology due to the interplay between QSE and CSE, which can be regulated by island thickness. It allows us to characterize the transition from the quantum to the classi-

cal growth regime, to identify the stability transition caused by quantum beating, and to deduce the critical surface energy difference,  $\sim 5$  meV. From the growth kinetics, we further show that the diffusion barriers on the Pb(111) surface oscillate with thickness in a periodicity of  $\sim 2$  ML, which is also ascribed to electron quantization.

Our experiments were performed in a molecular beam epitaxy system combined with an ultrahigh vacuum ( $\sim 5 \times 10^{-11}$  Torr) variable temperature STM. The Pb(111) islands were grown by depositing high purity (99.999%) Pb from a Knudsen cell on Si(111) substrates precleaned using standard flashing procedures.<sup>13</sup> During Pb deposition, the Si(111) substrates were held at 145 K. The STM manipulation was done by applying a voltage pulse of up to 10 V for several milliseconds at a surface site of interest. Immediately after the pulse, STM scanning was resumed to monitor the morphological evolution, with a typical tunneling current of  $\sim 20$  pA and a tip bias voltage of 1.5 V at variable temperatures from  $\sim 300$  to  $\sim 240$  K.

The as-grown Pb islands normally have flat-top geometries of low surface step energy but high quantized electron energy, as schematically shown in Figs. 1(i) and 1(l). The quantized electron energy can be lowered by growing one more atomic layer on top of the QSE-unfavored regions to make them more stable [Figs. 1(j) and 1(k)]. If these two effects are quantitatively comparable, the system is frustrated in terms of being unable to satisfy both QSE and CSE simultaneously. Remarkably, by applying an electric pulse using an STM tip, the island can be transformed between the CSE-favored flat-top and QSE-favored strip-top morphology in a controllable manner.

The scenario is shown by sequential STM images in Fig. 1. Figure 1(a) shows the original flat-top wedge island. After applying an electric pulse (+5 V to the STM tip), a new Pb layer forms spontaneously, starting from where the pulse was applied. The nucleation of the new layer is an electric-field-aided process and the Pb atoms supplying the growth come from the neighboring Pb islands, which has been discussed previously.<sup>7,10</sup> Interestingly, the initial pulse-induced growth is featured by a novel selective-strip flow defined by the

substrate steps buried underneath [Figs. 1(b)–1(d)]. The selective-strip flow growth was first reported by Okamoto *et al.*<sup>7</sup> The atomic layer grows only on the odd layer-number regions, leaving the original even layer-number regions unchanged. This strip-flow growth continues until all regions have even number of layers. The island by this point has transformed to a new state with the lowest quantized electron energy and the highest step energy [Figs. 1(d) and 1(j)]. If no additional pulse is applied, the island will recover its flat top by atom incorporation at the steps, which minimizes the step energy at the expense of the quantized electron energy (image not shown). In this way, each operation adds precisely one complete atomic layer of Pb atoms on the wedge.

Such island evolution can also display more intricate dynamics. We can suppress the flat-top recovery process by applying a second pulse just before it takes place, leading to a different growth pathway. Surprisingly, the second pulse triggers double-layer strip flow as shown in Figs. 1(e) and 1(f) and Fig. 1(k). In this case, QSE dominates causing two layers of atoms to grow simultaneously and the system always retains the lowest quantized electron energy. A similar double layer growth was first observed by Okamoto *et al.*<sup>7</sup> Again, when left alone, the growth will eventually proceed to restore the flat-top configuration [Figs. 1(g) and 1(h), and Fig. 1(l)].

QSEs are known to decay with oscillations with increasing film thickness.<sup>1,2</sup> Figure 2(a) shows the growth mode transition from the quantum to the classical regime taking place at the critical thickness of 26 ML (the wetting layers are included). This novel growth behavior of selective strip-flow followed by flat-top recovery (in the quantum regime) can be repeated many times as long as the island's thickness is smaller than the critical thickness [see the island's thinner side in Fig. 2(a)]. Above this critical value, the growth transforms into conventional step-flow mode (the classical regime), wetting the island's edge followed by vacancy island decay, which is dominated by minimizing step energy [see the island's thicker side in Fig. 2(a)].<sup>10</sup> Figure 2(b) shows another interesting phenomenon in the regime of 17–18 ML: for thicknesses smaller than 17 ML, selective strip-flow growth takes place on even-layer-number regions and step flow on the odd layer-number regions, whereas it is reversed for thicknesses larger than 18 ML. At both 17 and 18 ML, growth proceeds via step flow, which indicates that the QSE in this regime is insufficient to overcome the CSE. The critical thickness of ~26 ML for the quantum-classical transition and the stability switching between even and odd numbers of layers at 17–18 ML agrees quite well with the quantum beating pattern imposed on the envelope function of the surface energy.<sup>14–16</sup>

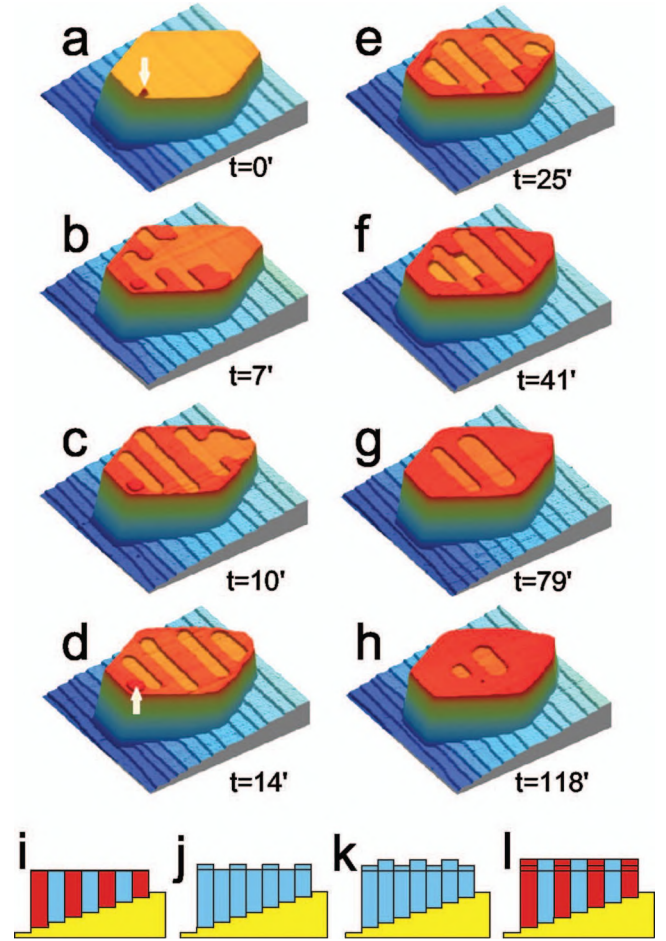


FIG. 1. (Color) A sequence of STM images (1000 nm  $\times$  1000 nm) recorded at room temperature showing the evolution of a Pb island on Si(111). (a) Original Pb island before STM manipulation. The thickness of Pb layers on top of each Si terrace increases successively from 4.5 to 7.3 nm, measured on top of the wetting layer. The arrow marks the position where the voltage pulse (+5 V) was applied to the STM tip. (b)–(d) Selective strip-flow growth turning odd-layer-number regions into even numbers of layers. (e)–(f) Double-layer strip growth maintaining the even number of layers. (g)–(h) Flat top recovery growth to reduce surface steps. (i)–(l) Side-view schematics showing the original island, selective strip-flow growth, double-layer strip growth, and flat-top-recovery growth, respectively. Blue indicates the QSE-favored even-layer-number regions, and red the QSE-unfavored-odd-layer-number regions.

To quantitatively analyze the critical transitions, we calculate the total free energies for the reduced quantum and classical growth modes shown in Figs. 2(c) and 2(d) as

$$E(\Theta) = \begin{cases} \Theta \left( E_C - E_Q + 2 \frac{n-2}{L} \lambda_S \right) + 4L\lambda_S, & \Theta < \frac{L^2}{2}, \\ \Theta \left( E_C + E_Q - 2 \frac{n}{L} \lambda_S \right) - L^2 \left( E_Q - 2 \frac{n}{L} \lambda_S \right) + L\lambda_S, & \Theta > \frac{L^2}{2}, \end{cases} \quad (1)$$



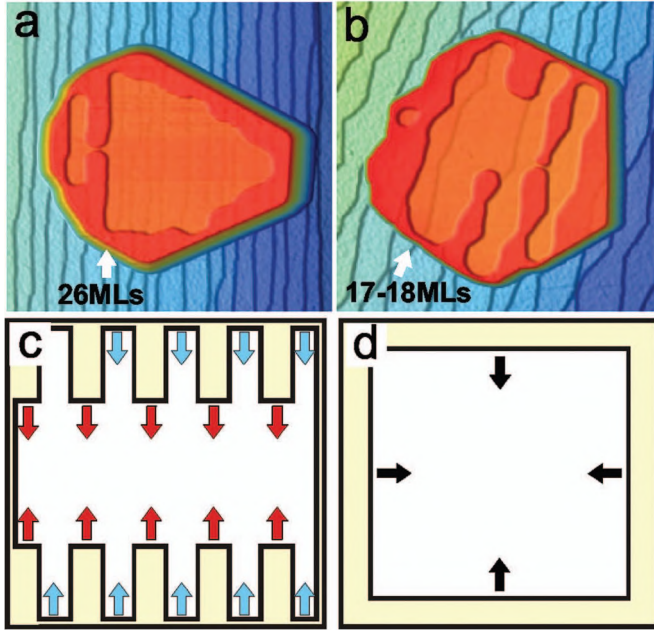


FIG. 2. (Color) (a) STM image (1000 nm  $\times$  1000 nm) illustrating the quantum-classical growth transition, the white arrow indicates the critical thickness of 26 ML. (b) STM image (1300 nm  $\times$  1300 nm) illustrating quantum beating in morphological dynamics, the arrow indicates the critical thicknesses of 17 and 18 ML. The thickness increases from left to right for Pb islands in both (a) and (b). (c) and (d) Schematic diagrams illustrating the quantum and classical growth mode, respectively. Red and blue arrows in (c) indicate the growth directions of the selective strip and the following flat-top recovery respectively, and black arrows in (d) indicate the growth directions for classical growth.

$$E(\Theta) = 4\sqrt{L^2 - \Theta}\lambda_s + \Theta E_C. \quad (2)$$

$E(\Theta)$  in (1) and (2) are total energies for the cases of Figs. 2(c) and 2(d), respectively, and  $\Theta$  is the growing layer's area (coverage).  $E_C$  is the average surface energy in the classical growth mode, and  $E_Q$  is the quantum correction of the surface energy due to QSE.  $\lambda_s$  is the free energy per unit step length. The original Pb wedge is assumed to be a square flat top with sides of length  $L$  covering  $n$  Si steps (thus, the average terrace width is  $L/n$ ). We define  $F(E_Q, n/L) \equiv E_Q - 2\lambda_s(n/L)$  as the effective difference of the QSE energy and the CSE energy, to characterize the growth behavior.  $F(E_Q, n/L) = 0$  indicates the transition from quan-

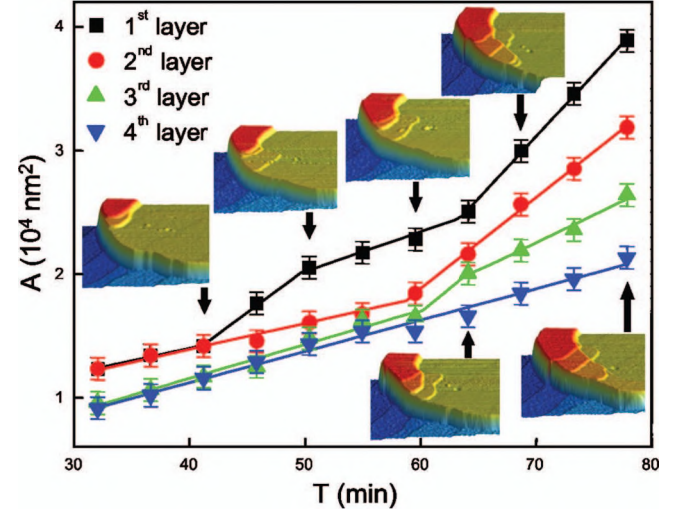


FIG. 3. (Color) Time evolution of four stacked Pb layers created by a voltage pulse of +7 V applied at  $t=0'$  to the STM tip. STM scanning was performed at  $\sim 240$  K. The first, second, third, and fourth layers are marked from bottom to up. Insets show the corresponding STM images (300 nm  $\times$  230 nm) of the growth fronts. The thickness of the original Pb island increases from right to left.

tum to classical growth. Quantitatively, the step energy of Pb(111) has been calculated to be 78 meV/ $\text{\AA}$  (Refs. 17 and 18). Taking the average terrace width as  $\sim 500$   $\text{\AA}$  [Fig. 1(a)], we estimate the critical surface energy difference between two consecutive layers (one an odd number of layers thick and the other an even number) to be  $\sim 5$  meV per unit cell, which is in reasonable agreement with the value reported recently,<sup>14,15</sup> considering the simplification made in the model and the sensitivity of electron confinement to interface structures.<sup>19</sup> Therefore, whether the triggered islands grow in quantum or classical regime is determined by energetics: quantum growth prefers on the thin films and classical growth the thick films. In the quantum growth regime, one may induce double-layer growth, short-cutting the flat-top recovery process. Island growth is also strongly related to the kinetic pathways: to initiate QSE-driven growth, a high nucleation barrier needs to be overcome, which is realized here with the help of STM manipulation.<sup>20–25</sup> Since both the QSE-mediated surface energy and the step energy are not related to temperature, the thickness for the growth mode transition and beating node do not change apparently with temperature. However, to trigger the growth, enough thermal energy is necessary to activate the diffusion of Pb atoms.

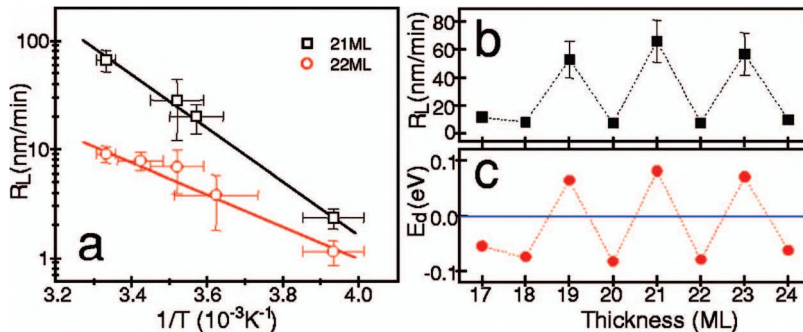


FIG. 4. (Color) (a) Arrhenius plots for the selective strip growth at 21 ML and flat-top-recovery growth at 22 ML. (b) Line rate versus thickness obtained at  $\sim 300$  K. (c) Relative effective diffusion barrier versus thickness.

We further investigate the growth kinetics by triggering multilayers with a +7 V pulse to the STM tip. Figure 3 shows the temporal evolution of the “step-crossing” growth of four stacked layers at  $\sim 240$  K (Ref. 26). The growth rate of each layer is different and also changes in regions of different thickness. Once the growth fronts enter the QSE-unfavored terraces, the growth rate becomes higher (the first layer at 41 and 64 min in Fig. 3). In contrast, the growth rate is slowed down in the QSE-favored terraces (the first layer at 50 min, the third layer at 64 min, and the entire fourth layer). When the growth front of the third layer catches up with that of the second layer on the QSE-unfavored terraces (at 60 min), it turns into double-layer flow. Such intriguing oscillatory behavior in growth rates further confirms that selective strip growth is promoted by the QSE rather than the elastic strain effect.

The growth area for selective strip growth and flat-top recovery is found to be linearly dependent on time, resulting in a constant growth rate. Deviations from linearity are found only at the end of flat-top recovery growth when two opposite fronts meet. This is because the growth rate is linearly dependent of the length of growth front, which remains unchanged for such substrate-step-confined growth. We assume a linear rate (growth rate divided by the terrace width) on the terrace of  $N$  ML  $R_L(N) = \nu \exp\{-\frac{E_d(N)}{k_B T}\} \exp\{-\frac{E_Q(N) + \Delta\mu}{k_B T}\}$ , where  $\nu$  is the hopping frequency that is supposed constant and  $E_d(N)$  is the effective diffusion barrier.  $E_Q(N)$  is the QWS-mediated relative surface energy and  $\Delta\mu_C$  is the classical part of chemical potential difference. The growth direction is along the Si steps. Figure 4(a) shows the Arrhenius plots for selective strip growth at 21 ML and flat-top-recovery growth at 22 ML. Assuming the relative surface energy is  $\sim 20$  meV,<sup>14</sup> the effective diffusion barrier  $E_d(21)$  is determined to be  $\sim 0.15$  ( $\pm 0.03$ ) eV higher than  $E_d(22)$ , which

means that the diffusion barrier is also mediated by quantized electrons.<sup>27</sup> However, this value is simply too large, implying that other kinetic factors such as the barrier for Pb adatoms jumping from the sidewall to the top of the islands and the additional Ehrlich-Schwoebel barrier, are also possibly modified by QSEs to be thickness-dependent. Figure 4(b) shows the linear rate  $R_L$  of single layer on the terraces from 17 to 24 ML at  $\sim 300$  K. Evidently, growth rates at different thicknesses oscillate with  $\sim 2$  ML periodicity. Figure 4(c) shows the relative effective diffusion barriers for terraces from 17 to 24 ML deduced from the growth rate oscillations. The oscillatory behavior of the effective diffusion barrier is consistent with the quantized electronic energy in Pb(111) films.<sup>14</sup> Therefore, the diffusion barrier is confirmed to be modified by quantized electrons and oscillates with a periodicity of 2 ML, which is responsible for the growth rate oscillations.

In conclusion, we have demonstrated Pb island growth driven alternately by QSE and CSE in a controlled manner. We showed that local kinetic pathways play an important role in morphological evolution. A quantitative analysis was also given for the transition from the quantum to the classical growth regime and the reverse dynamics transition with increasing film thickness. By investigating these kinetic processes, we conclude that the diffusion barriers are also mediated by quantized electrons and display 2 ML periodic oscillations. This work provides a potential approach to tailor nanostructures precisely via manipulation of quantum size effects.

Our work at IOP was supported by the National Science Foundation of China, and Ministry of Science and Technology of China. F.L. acknowledges support from NSF-DMR 0307000. S.-C.L. and P.S.W. acknowledge support from AFOSR.

\*Corresponding author. Email address: jfjia@aphy.iphy.ac.cn

<sup>1</sup>T.-C. Chiang, *Surf. Sci. Rep.* **39**, 183 (2000).

<sup>2</sup>J. J. Paggel, T. Miller, and T.-C. Chiang, *Science* **283**, 1709 (1999).

<sup>3</sup>A. R. Smith, K.-J. Chao, Q. Niu, and C.-K. Shih, *Science* **273**, 226 (1996).

<sup>4</sup>Z. Zhang, Q. Niu, and C.-K. Shih, *Phys. Rev. Lett.* **80**, 5381 (1998).

<sup>5</sup>I. B. Altfeder, K. A. Matveev, and D. M. Chen, *Phys. Rev. Lett.* **78**, 2815 (1997).

<sup>6</sup>W. B. Su, S. H. Chang, W. B. Jian, C. S. Chang, L. J. Chen, and T. T. Tsong, *Phys. Rev. Lett.* **86**, 5116 (2001).

<sup>7</sup>H. Okamoto, D. Chen, and T. Yamada, *Phys. Rev. Lett.* **89**, 256101 (2002).

<sup>8</sup>V. Yeh, L. Berbil-Bautista, C. Z. Wang, K. M. Ho, and M. C. Tringides, *Phys. Rev. Lett.* **85**, 5158 (2000).

<sup>9</sup>Y. Guo, Y.-F. Zhang, X.-Y. Bao, T.-Z. Han, Z. Tang, L.-X. Zhang, W.-G. Zhu, E. G. Wang, Q. Niu, Z. Q. Qiu, J.-F. Jia, Z.-X. Zhao, and Q.-K. Xue, *Science* **306**, 1915 (2004).

<sup>10</sup>C.-S. Jiang, S.-C. Li, H.-B. Yu, D. Eom, X.-D. Wang, Ph. Ebert,

J.-F. Jia, Q.-K. Xue, and C.-K. Shih, *Phys. Rev. Lett.* **92**, 106104 (2004).

<sup>11</sup>K. Thürmer, J. E. Reutt-Robey, and E. D. Williams, *Surf. Sci.* **537**, 123 (2003).

<sup>12</sup>Y. Han, J. Y. Zhu, F. Liu, S.-C. Li, J.-F. Jia, Y.-F. Zhang, and Q.-K. Xue, *Phys. Rev. Lett.* **93**, 106102 (2004).

<sup>13</sup>S.-C. Li, J.-F. Jia, R.-F. Dou, Q.-K. Xue, I. G. Batyrev, and S. B. Zhang, *Phys. Rev. Lett.* **93**, 116103 (2004).

<sup>14</sup>P. Czoschke, H. Hong, L. Basile, and T.-C. Chiang, *Phys. Rev. Lett.* **93**, 036103 (2004).

<sup>15</sup>M. H. Upton, C. M. Wei, M. Y. Chou, T. Miller, and T.-C. Chiang, *Phys. Rev. Lett.* **93**, 026802 (2004).

<sup>16</sup>Y.-F. Zhang, J.-F. Jia, T.-Z. Han, Z. Tang, Q.-T. Shen, Y. Guo, Z. Q. Qiu, and Q.-K. Xue, *Phys. Rev. Lett.* **95**, 096802 (2005).

<sup>17</sup>P. J. Feibelman, *Phys. Rev. B* **62**, 17020 (2000).

<sup>18</sup>M. Nowicki, C. Bombis, A. Emundts, and H. P. Bonzel, *Phys. Rev. B* **67**, 075405 (2003).

<sup>19</sup>C. M. Wei and M. Y. Chou, *Phys. Rev. B* **66**, 233408 (2002).

<sup>20</sup>P. S. Weiss and D. M. Eigler, *Phys. Rev. Lett.* **69**, 2240 (1992).

<sup>21</sup>D. M. Eigler and E. K. Schweizer, *Nature (London)* **344**, 524

- (1990); J. A. Stroscio and D. M. Eigler, *Science* **254**, 1319 (1991).
- <sup>22</sup>T. C. Shen, C. Wang, G. C. Abeln, J. R. Tucker, J. W. Lyding, Ph. Avouris, and R. E. Walkup, *Science* **268**, 1590 (1995).
- <sup>23</sup>S.-W. Hla, L. Bartels, G. Meyer, and K.-H. Rieder, *Phys. Rev. Lett.* **85**, 2777 (2000).
- <sup>24</sup>B. C. Stipe, M. A. Rezaei, and W. Ho, *Science* **280**, 1732 (1998).
- <sup>25</sup>J. K. Gimzewski and C. Joachim, *Science* **283**, 1683 (1999).
- <sup>26</sup>Once a nucleus is created near the edge of the wedge by STM, atom incorporation to the nucleus leads to the first-stage fast growth alongside the wedge edge. After a closed ring forms along the edge, the second-stage growth requires atoms to overcome an additional wedge-edge barrier.
- <sup>27</sup>C. A. Jeffrey, E. H. Conrad, R. Feng, M. Hupalo, C. Kim, P. J. Ryan, P. F. Miceli, and M. C. Tringides, *Phys. Rev. Lett.* **96**, 106105 (2006).